A Full-Featured, Enhanced Cost Function to Mitigate Motion Sickness in Semi- and Fully-autonomous Vehicles

Isa Moazen and Paolo Burgio
HiPeRT Lab., University of Modena and Reggio Emilia, Italy

Keywords: Motion Sickness, Autonomous Driving, Comfort, Model-Predictive Control, Cost-function, Embedded Control Systems.

Abstract: Current full- and semi- Autonomous car prototypes increasingly feature complex algorithms for lateral and longitudinal control of the vehicle. Unfortunately, in some cases, they might cause fussy and unwanted effects on the human body, such as motion sickness, ultimately harnessing passengers' comfort, and driving experience. Motion sickness is due to conflict between visual and vestibular inputs, and in the worst case might causes loss of control over one’s movements, and reduced ability to anticipate the direction of movement. In this paper, we focus on the five main physical characteristics that affect motion sickness, including them in the function cost, to provide quality passengers' experience to vehicle passengers. We implemented our approach in a state-of-the-art Model Predictive Controller, to be used in a real Autonomous Vehicle. Preliminary tests using the Unreal Engine simulator have already shown that our approach is viable and effective, and we implemented and evaluated using Motion Sickness Dose Value and Illness Rating and then tested it in an embedded platform. We implemented it on our embedded platform, NVIDIA Jetson AGX Xavier that is representative of the next-generation AV Domain Controller.

1 INTRODUCTION

In semi- and full AVs, vehicle control shall consider passengers’ stress, and not decrease their level of comfort (Elsner, 2018). It was proven that a tight relationship exists between comfort and trust, as well as the acceptance of automated vehicles (Bellem et al., 2018).

The mostly known comfort issues for the passengers is probably Motion Sickness. Its common symptoms are: headache, pallor, sweating, nausea, vomiting, and disorientation, and they can be measured by Physiological signals, Vestibule Ocular Reflex (VOR) parameters, and Posture stability. There are several ways to mitigate this, such as instance visual cues, Posture and vehicle controllability, and Immersive Experience (Iskander et al., 2019).

Motion is primarily sensed by the organs of balance located in the inner ear and our eyes, which are mainly or uniquely sensitive to accelerations. The vestibular section of the inner ear is partly comprised of three semi-circular canals that detect head angular acceleration. The main issue stems from the fact that our bodies are not used to low-frequency oscillating motion, and our “biological IMUs” are highly sensitive to this. In carsickness, the lateral accelerations (sway) in the low-frequency bands (0.1-0.5 Hz) are most relevant and their effects increase in higher accelerations. In general, researchers proved (Diels, 2014) that it might happen when the frequency is below 1 Hz.

The potential sources of AV motion sickness are variation in horizontal and vertical acceleration, posture instability, loss of controllability and loss of anticipation of motion direction, Head downward inclination, and lack of synchronization between virtual motion and the vehicle motion profile (Iskander et al., 2019). Although motion sickness is most frequently caused by a conflict between visual and vestibular inputs, loss of control over one’s movements and reduced ability to anticipate the direction of movement are also important in the etiology of motion sickness (Sivak and Schoettle, 2015). All three factors, to varying degrees, are more frequently experienced by vehicle passengers than by drivers, who rarely experience motion sickness (Sivak and Schoettle, 2015). Possible counter measures can be categorized into two groups: prevention solutions and mitigation solutions.

Moazen, I. and Burgio, P.
A Full-Featured, Enhanced Cost Function to Mitigate Motion Sickness in Semi- and Fully-autonomous Vehicles.
DOI: 10.5220/0010446604970504
In *Proceedings of the 7th International Conference on Vehicle Technology and Intelligent Transport Systems (VEHITS 2021)*, pages 497-504
ISBN: 978-989-758-513-5

Roughly speaking, the degree of motion sickness may be predicted by an acceleration frequency weighting that is independent of frequency from 0.0315 to 0.25 Hz and reduces at 12 dB per octave (i.e., proportional to displacement) in the range 0.25 to 0.8 Hz (Iskander et al.., 2019).

We contribute to research with the original design of a control software component for AVs that minimizes the most important costs. In this paper, we used an Adaptive Model Predictive Control (AMPC) that can estimate and update the model in real-time along with five constraints to build our cost function to minimize.

We have chosen the constraints that are relevant to Motion Sickness and comfort, either direct or indirect. Acceleration frequency is one of the constraints that directly affects the Motion Sickness and the range of Frequency in which Motion Sickness occurs is in 0.0315<F<0.8 Hz (Donohew & Griffin, 2004). Speed limitation is not directly related to Motion Sickness level. However, as the speed goes up, Acceleration Frequency for the speed regulation will arise. Therefore, we consider a speed limitation based on our Acceleration Frequency. The European New Car Assessment Program (Euro NCAP) performed standardizing tests on different autonomous vehicles with a constant speed of 20 – 60 km/h (Standard, 1987). We also consider a threshold of acceleration because it affects both Motion Sickness and Comfort driving (Standard, 1987). It is also one of the factors that increase Motion Sickness Dose Value (MSDV). Therefore, having the limitation with an appropriate planner can lower the MSDV and raise comfort. We also consider the distance from the next vehicle to brake with a minimum acceleration, as we discussed before. In particular, with higher distance from the next vehicle, we require a lower braking acceleration. Finally, since the lateral acceleration is the other important source in MSDV (Donohew & Griffin, 2004), we need a lane keeper to reduce our lateral accelerations to a minimum quantity.

The system is tested on MATLAB/Simulink (MATLAB, 2020) and then implemented on an NVIDIA Xavier AGX. We evaluate our work based on ISO 2631-1 (Standard, 1987) which a measure of the probability of nausea that is called motion sickness dose value (MSDV) and a simple linear approximation between MSDV and mean passenger named illness rating (IR) are considered as the evaluation methods.

In the following sections, we first review the state-of-the-art in motion sickness and MPC controller. Then we describe the details of our controller. Finally, we show our implementation, and discuss experimental results with respect to the reference metrics of motion sickness.

2 MOTION SICKNESS IN AV LITERATURE

Several works are done for the motion sickness mitigation and minimization in the recent years. In (Elsner, 2018) a library of cost functions, consisting of progress, comfort, and safety costs, is used to evaluate the strategies generated by the three modules distance keeper, lane selector, and merge planner. In (Sivak & Schoettle, 2015), two strategies for reducing the visual-vestibular conflict while watching videos are investigated. One approach imposes visual stimuli on or around the video screen to mimic the perceived motion and forces of the moving vehicle. The other method involves controlling the position of displayed images in synchronization with vehicle motions and passenger's head motions produced by vehicle acceleration/deceleration, thus providing a video that appears to be stabilized in relation to the movement of the vehicle. In (Lambert et al., 2019), a method is proposed for generating optimal Path Planning with Clothoid Curves for passenger comfort, and their cost is based on the squared distance along the curve, made up of the first clothoid length, the second clothoid length, and the straight line to the goal at the end. An application of Motion Planning is presented in (Htike et al., 2020) in order to minimize MSDV in self-driving vehicles. Most of the works are considering some parameters but not all to minimize. However, since the Motion Sickness occurs based on different sources, to minimize it, we need to consider all of the Motion Sickness sources. In this manner, we require to distinguish the actual direct and indirect sources and try to minimize or remove them. Furthermore, it is essential to consider comfort driving while minimizing the Motions Sickness rate. To overcome these important factors, as opposite to the other works, our work considers the direct and indirect sources of Motion Sickness and tries to minimize them all in a single cost function to enhance passengers' comfort.

Considering recent AMPC implementations in autonomous driving, concentrating on their cost functions, there are several efforts. In (Easa & Diachuk, 2020), an adaptive model predictive control with three constraints, Lane Change-Related Constraint, Location in Opposite Lane Constraint, and Maneuver Completion, is applied for tracking the references being generated for the Autonomous Vehicles on Two-Lane Highways. In (Shi et al., 2020), they constructed an adaptive model predictive control trajectory tracking system with the four constraints. In (Wu et al., 2020), an adaptive model predictive control (AMPC) scheme is developed to improve the yaw stability for four-wheel-independently actuated electric vehicles by minimizing the total longitudinal forces of all wheels. In (Luan et al., 2020), the side slip angle of the centre of mass and the side slip angle of the tire as hard constraints and the lateral acceleration as a soft constraint are considered to propose an Adaptive Model Predictive Control for Uncertain model (UMAMPC) algorithm to predict control variables for the next sampling time and alleviate the target angle discontinuity. In (Geng and Liu, 2020), they develop a fault tolerant path tracking control algorithm through combining the adaptive model predictive control algorithm for lateral path tracking control and Kalman filtering approach with two states chi-square detector and residual chi-square detector for detection and identification of sensor fault in autonomous vehicles by using the incremental constraint of tire and the incremental constraint of lateral acceleration.

In all of the above works, that are proposed for controlling the autonomous vehicles by AMPC, below than five constraints are used. In this work, we use five constraints in an AMPC that minimize the MSDV with consideration of comfort.

3 CONTROL SYSTEM

To design the controller, we defined a Vehicle Model and used the tire forces to specify our state space. Then, we entered our state space in AMPC and defined our constraints in it.

3.1 Vehicle Model

For an MPC control design, we require to define our Vehicle Model. It was found that the vehicle side slip angle is less than 1◦ in the highway autonomous or manoeuvre driving under clothoid constraints (Kang et al., 2014). Thus, it is considered that the tire slip angle is also negligible under highway driving conditions, including cases employing an advanced driver assistant system (ADAS). It makes it possible to use a standard dynamic "bicycle model" (Rajamani, 2011) to describe the Vehicle Dynamics. Such as a recent work (Antonelli et al., 2019) that uses the higher speed until 35 m/s (126 km/h) with a bicycle dynamic model, we use a bicycle dynamic model for our tests between the speed of 0 km/h to 80 km/h and we use them in our first scenario. In the bicycle model, the two left and right wheels are represented by one single wheel. The model is derived assuming both front and rear wheels can be steered by δf and δr angles and the distances of front and rear wheels are a and b. The model neglects roll and pitch motions. The Motion of the vehicle is represented by X, Y and ψ. Figure 1 depicts a diagram of the vehicle model, which has the following longitudinal, lateral, and turning or yaw equations:

$$m\ddot{x} = mr\dot{y} + Fx_f + Fx_r \tag{1}$$

$$m\ddot{y} = -mr\ddot{x}\dot{\psi} + Fy_f + Fy_r \tag{2}$$

$$I_{zz}\ddot{\psi} = aF_{yf} - bF_{yr} \tag{3}$$

The vehicle's equations of motion in an absolute inertial frame are

$$\dot{Y} = \dot{x}\sin\psi + \dot{y}\cos\psi \tag{4}$$

$$\dot{X} = \dot{x}\cos\psi - \dot{y}\sin\psi \tag{5}$$

Longitudinal and lateral tire forces lead to the following forces acting on the centre of gravity:

$$\mathrm{Fy} = \mathrm{Fl}\sin\delta + \mathrm{Fc}\cos\delta, \tag{6}$$

$$\mathrm{Fx} = \mathrm{Fl}\cos\delta - \mathrm{Fc}\sin\delta. \tag{7}$$

Tire forces for each tire are

$$\mathrm{Fl} = \mathrm{fl}(\alpha, s, \mu, \mathrm{Fz}), \tag{8}$$

$$\mathrm{Fc} = \mathrm{fc}(\alpha, s, \mu, \mathrm{Fz}), \tag{9}$$

where α is the slip angle of the tire and s is the slip ratio. The tire model is considered as indicated in (Filip, 2018) velocities, respectively, are expressed as

$$\mathrm{vl} = \mathrm{vy}\sin\delta + \mathrm{vx}\cos\delta, \tag{10}$$

$$\mathrm{vc} = \mathrm{vy}\cos\delta - \mathrm{vx}\sin\delta, \tag{11}$$

and

$$v_{yf} = \dot{y} + a\dot{\psi} \qquad v_{yr} = \dot{y} - b\dot{\psi}, \tag{12}$$

$$v_{xf} = \dot{x} \qquad v_{xr} = \dot{x}. \tag{13}$$

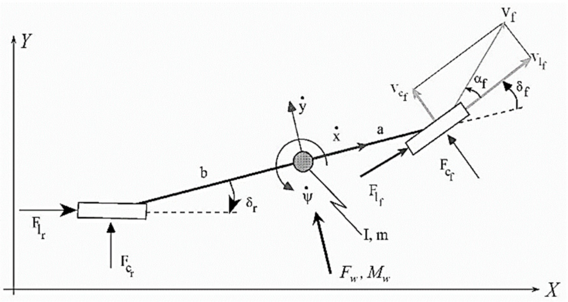

Figure 1: Bicycle Model of the Vehicle.

If we consider δr =0, then:

$$\ddot{x} = r\dot{y} + \frac{Flf\ cos(\delta f) - Fcfsin(\delta f) + Flr}{m} \quad (14)$$

$$\ddot{y} = -r\dot{y} + \frac{Flf\ sin(\delta f) + Fcfcos(\delta f) + Flr}{m} \quad (15)$$

$$\dot{r} = \frac{a(Flf\ sin(\delta f) - Fcfcos(\delta f)) - bFcr}{Izz} \quad (16)$$

Using the equations (1)-(16), the nonlinear vehicle dynamics will have the states of $[\dot{X} \quad \dot{Y} \quad \dot{\psi} \quad \dot{v}x \quad \dot{v}y \quad \dot{r}]$.

3.2 Adaptive Model Predictive Control System

MPC (Muske & Rawling, 1993) is a method for process control that actively uses the dynamic model of the system. If the nonlinearity is high, however, MPC performance could deteriorate. In this case, one can use an AMPC that constantly predicts the new operating conditions. (Önkol and Kasnakoğlu, 2018).

An adaptive MPC algorithm is designed by using the recursively-identified state-space models with dynamic adjustments of MPC constraints and objective function weights (Hajizadeh et al., 2020). Adaptive MPC controllers adjust their prediction model at run time to compensate for nonlinear or time-varying plant characteristics. Furthermore, Adaptive control for constrained systems has mainly focused on improving performance with the adapted models, while the constraints are satisfied robustly for all possible model realizations and the worst disturbance bounds (Aswani et al., 2013). In this paper, we used an Adaptive MPC to update our state-space online and get the linear part of our nonlinear system. This approach is implemented with the most important costs that we wanted to control.

In AMPC, the controller uses the time-varying Kalman filter (TVKF) instead of the static one to provide consistent estimation with the updated plant dynamics. The TVKF approach can be expressed as follows

$$L_K = \left(A_k P_{k|k-1} C_{m,k}^T + N\right)\left(C_{m,k} P_{k|k-1} C_{m,k}^T + R\right)^{-1}$$
$$M_K = P_{k|k-1} C_{m,k}^T \left(C_{m,k} P_{k|k-1} C_{m,k}^T + R\right)^{-1} \quad (17)$$
$$P_{k|k+1} = A_k P_{k|k-1} A_k^T - \left(A_k P_{k|k-1} C_{m,k}^T + N\right) L_k^T + Q$$

In equation (17), Q, R, and N matrices are constant covariance matrices, and Ak and Cm, k are matrices depicting the state-space description of the system. The Pk|k−1 is the state estimate error covariance matrix at k constructed from the information from time k−1. TVKF is constructed to update regularly the L and M matrices with the updated plant dynamics.

3.2.1 Constraints

The Model Predictive Control can directly include constraints in the computation of the control moves which leads to linear program (LP) or quadratic program (QP) to be solved at each sampling instance, with the constraints written directly as constraints in the LP/QP.

The MPC algorithm solves a quadratic optimization problem at each time interval. The solution of the problem determines the so-called manipulated variables (MV), which are essentially the input variables adjusted dynamically to keep the controlled variables (CV) at their set-points. The AMPC approach follows the same cost optimization algorithm as MPC with the cost function

$$J_y(z_k) = \sum_{j=1}^{n_y} \sum_{i=1}^{p} \left\{ \frac{w_{i,j}^j}{s_j^y} \left(r_j(k+i|k) - y_j(k+i|k) \right) \right\}^2 \quad (18)$$

where k represents the current control interval, p is the prediction horizon (interval number), n_y is the number of plant output variables, z_k is the quadratic problem (QP) selection which is depicted as the formula $z_k^T = [u(k|k)^T \ u(k+1|k)^T \ldots u(k+p-1|k)^T\ k]$, $y_j(k+i|k)$ is the jth CV at the ith prediction horizon step, $r_j(k+i|k)$ is the ith references variable at the ith prediction horizon step, s_j^y is the scale factor for the jth plant output variable, and $w_{i,j}^j$ is the tuning weight coefficient reflecting the relative importance of the plant output variable. Among these variables n_y, s_j^y, p, and $w_{i,j}^j$, are determined during the controller design and stay constant.

Acceleration Frequency. The range of Frequency in which Motion Sickness is tested in 0.0315<F<0.8 Hz. However, the maximum Motion sickness occurs at 0.2 Hz (Donohew & Griffin, 2004). So we fixed frequency at 0.2 Hz which means T= 5 s. In particular, that we prevent inserting acceleration every 5 seconds.

Speed Limit. As discussed, the test speed is in the range of 20 – 60 km/h (Standard, 1987). Since we need to consider having acceleration and braking in our work, we raised this limitation to 0 - 80 km/h and in our tests, we consider these values.

Acceleration Limit. Acceleration limitation is an important source for comfort and the different level of comfort is measured based on it (Standard, 1987).

Based on ISO 2631 (Standard, 1987) for determination of acceleration, the best range of the acceleration is <0.315 m/s2 that is named not uncomfortable. In this standard, the best range of acceleration is <1 m/s2 that is fairly uncomfortable and it is the border of the uncomfortable range of measurements. So we maintain this range.

Distance to the Front Vehicle. With a higher distance from the next vehicle, we decrease the braking acceleration. It means that we will have more time to plan smooth braking, with the consideration of our acceleration limit, and it lowers the MSDV. There is a Two-Second Distance rule from the next vehicle (Road Safety Authority, 2011). The mean deceleration is 2.5 m/s2 (Yimer et al., 2020) and our deceleration should not exceed 1 m/s2. Therefore, we raised the distance to Five-Seconds Distance to fulfil these requirements.

Lane Keeper. As discussed, we have high importance in lateral acceleration to minimize the MSDV. Therefore, our system maintains the boundaries and controls the Y as the centre of the road lines. It is obtained by having a reference Y of the road and try to follow it. In the results, we show that our controller follows it properly.

3.3 Motion Sickness Evaluation

The total MSDV resulted from lateral and longitudinal motion is given as (Standard, 1987):

$$\text{MSDV}=\sqrt[2]{\int_0^T (a_{x,w}\,(t))^2} + \sqrt[2]{\int_0^T (a_{y,w}\,(t))^2} \qquad (19)$$

where ax,w(t) and ay,w(t) are the frequency weight acceleration in the longitudinal and lateral direction.

$$a_{x,w}\,(t) = a_x\,(t) \times W_f \qquad (20)$$

$$a_{y,w}\,(t) = a_y\,(t) \times W_f \qquad (21)$$

where ax(t) and ay(t) are the longitudinal and lateral acceleration. Wf is the weighting factor defined in British Standard 6841 (Standard, 1987) for evaluating low frequency motion with respect to motion sickness. From the standards (Standard, 1987), (Anon, 1997), a simple linear approximation between MSDV and mean passenger illness rating is given as:

$$\text{IR} = \text{K} \times \text{MSDV} \qquad (22)$$

where IR is predicted illness rating and K is an empirically derived constant. The illness rating value is divided into four levels; 0 indicates feeling fine, 1 indicates slightly unwell, 2 indicates quite ill, and 3 indicates absolutely dreadful (Standard, 1987), (Anon, 1997).

4 IMPLEMENTATION

The system was tested in MATLAB/Simulink (MATLAB, 2020) and then implemented by an NVIDIA Xavier AGX. This platform is representative of next-generation AV Domain Controller where AD software components, such as our controller, will execute.

To verify the validity of the proposed AMPC controller. CarSim (Mechanical Simulation Corporation, 2020) is used to provide a vehicle dynamics model and MATLAB/Simulink is mainly for providing control function.

Two different scenarios, straight and turn, were tested. The scenarios were designed in drivingScenarioDesigner and tested by using Unreal Engine (Epic Games, 2019) for the visualization of the output.

4.1 Scenarios

Since the MSDV is mainly a result of the lateral and longitude accelerations, we require to define the scenarios based on the existence of longitudinal acceleration, braking, and lateral acceleration. Therefore, we define a straight scenario that has the longitudinal acceleration and braking, and a turn scenario that has longitudinal and lateral accelerations.

4.1.1 Straight Road

In the straight scenario, we made a velocity profile. As it has shown in Figure 2, there were two vehicles in the scenario that the front vehicle (the truck) had 60 km/h speed and our vehicle model was 200 meters back of this vehicle with 80 km/h.

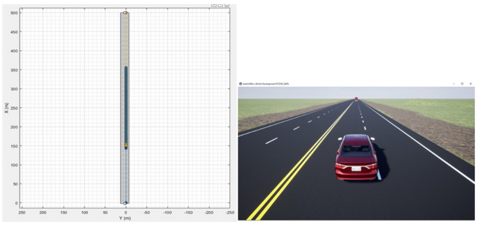

Figure 2: Our scenario in the drivingScenarioDesigner schematic in MATLAB.

4.1.2 Turn

We designed the other scenario for a comparison between our method and the other works. This scenario consists of different turns as shown in Figure 3. The speed limit of this scenario is between 0 to 40 km/h and at the first, the vehicle reaches the 40 km/h with our acceleration limitation that we discussed in constraints.

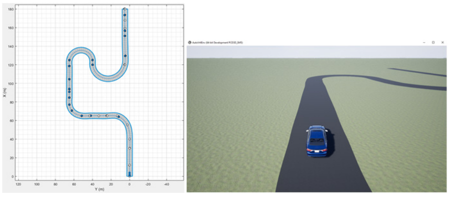

Figure 3: The Scenario visualization in Unreal Engine.

4.2 Adaptive Model Predictive Controller Design

We designed our AMPC using mpcDesigner (MATLAB, 2020) and Simulink. For each time step, our controller updated to make new states for the next prediction horizon. In Simulink, as shown in Figure 4, we used the Adaptive MPC block for this implementation which in it, the constraints and the MPC parameters are attached to it by mpcDesigner tool. The different blocks are to build the requirements of the Adaptive MPC block. We also brought our reference scenarios as discussed before. The prediction horizon considered as 10 seconds and the control horizon was 5 seconds with the sample time of 0.1 seconds. The tuning of weights was done by mpcDesigner tuning tool for closed-Loop Performance and State Estimation along with considering the system stability. The constraints, as discussed before, were defined in our controller using the mpcDesigner tuning tool.

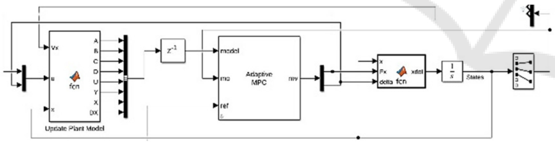

Figure 4: The Simulink implementation of Adaptive MPC.

4.3 Simulator

The system is tested with the Unreal Engine simulator (Epic Games, 2019) which connects to the Simulink. Our simulator considered the scenario data made by drivingScenarioDesigner, and added the output of the system to visualize and evaluate our system.

4.4 Embedded Platform

The target embedded platform, NVIDIA Jetson AGX Xavier is representative of the next-generation AV Domain Controller. This platform with a GPGPU of 512-core Volta with Tensor Core and a CPU of ARM 8-core v8.2 64-bit is an appropriate choice for the AD systems.

To have a realistic implementation, we can't rely on the Matlab/Simulink implementatn, and we utilized embedded coder of MATLAB/Simulink to convert our algorithm into C++ source code, which is then compiled for the target platform.

5 RESULTS AND DISCUSSION

Firstly, we calculated our results regarding of the first scenario, Straight scenario. Then, we investigated the results of the second scenario which is Turn. Finally, we tried to understand our timing results in the embedded platform to be able to use it along with other infrastructures.

We evaluated the scenarios by MSDV and IR then we compared our work with the latest works in this area. Our results shown different advantages compared to the previous approaches.

5.1 Results of the Scenarios

5.1.1 Straight Road

The straight scenario included two vehicles and a velocity profile. Our vehicle was behind a truck that was slightly far. It started from 0 and reached 80 km/h (22.22 m/s) and as soon as founded the distance of 5 seconds, it started slowing down to maintain the 5 seconds of the distance. Afterwards, it followed the truck by the truck's velocity. As shown in Figure 5, Figure 6, and Figure 7, the output of our controller follows the base-line with a small error.

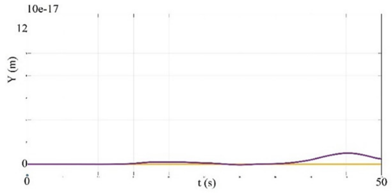

Figure 5: The scenario (blue) and our (orange) Y.

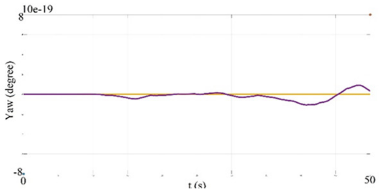

Figure 6: The scenario (blue) and our (orange) Yaw angle.

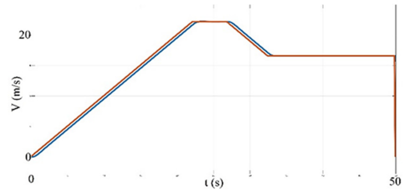

Figure 7: The scenario (orange) and our (blue) Velocity.

5.1.2 Turn

In the turn scenario, we maintained the acceleration limitation based on AMPC algorithm designed by Simulink and mpcDesigner. Figure 8, Figure 9, and Figure 10 show the results.

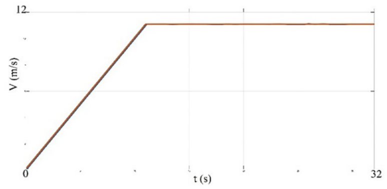

Figure 8: The scenario (orange) and our (blue) Velocity.

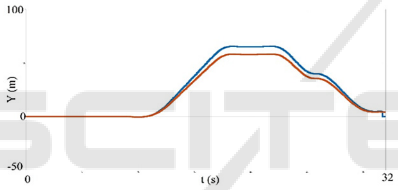

Figure 9: The scenario (blue) and our (orange) Y.

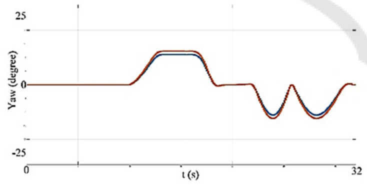

Figure 10: The scenario (blue) and our (orange) Yaw angle.

5.2 MSDV and IR Analysis

Our evaluation is based on MSDV and IR. IR generally increases overtime during a motion sickening stimulus (Reason & Graybiel, 1969). In (Standard, 1987), IR is considered as 0 when the passenger feels fine, 1 with a feeling of slightly unwell, 2 as quite ill, and 3 when the passenger is absolutely dreadful. As shown in Table 1, the output of the system more than having a small amount of IR which almost is zero, it has a comparison between the minimum IR of the previous work.

Table 1: The results of the IR evaluation.

Scenario	Time (s)	IR (min)
Straight	50	0.07
Turn	32	0.0017
Turn in (Htike et al., 2020)	29.73	0.044

Table 1 shows that the IR of the Turn scenario is much lower than the straight one. It is exactly what we expected considering the accelerations used in both scenarios since the Turn scenario has a much lower time of accelerating.

The results show that our performance is better since we try to use the acceleration as small as we can and we try to make it limited to 1 m/s2. Furthermore, our planner can make an IR near to zero. Therefore, it has a fine feeling according to (Standard, 1987).

5.3 Embedded Platform Performance

When running on the production-like embedded domain controller, our controller achieves 8.7 FPS, making it suitable to interact with the other AV components.

6 CONCLUSIONS

In this paper, we showed that by having a complex cost function with an emphasis on Motion Sickness Mitigation and consideration of comfort, we can achieve a smooth controller that does not make people sick. This work showed that the AV can have an algorithm for Motion Sickness mitigation along with the other tasks and make the AV more reliable than before.

For the next works, we can add other necessary features of AV such as LiDAR to detect and import the data for the Motion Sickness Mitigation Algorithm. It can finally be an algorithm which is used with the other infrastructures.

We also plan to adopt more complex vehicle models, such as the kinematic and dynamic model, to validate our approach at highest speeds (i.e., > 150km/h), and to possibly include other classes of vehicles, such as busses and coaches, which potentially issue Motion Sickness much more than cars.

ACKNOWLEDGEMENTS

This work was supported by the Prystine Project, funded by Electronic Components and Systems for European Leadership Joint Undertaking (ECSEL JU) in collaboration with the European Union's H2020 Framework Programme and National Authorities, under grant agreement n° 783190.

REFERENCES

Anon, B. (1997). Mechanical vibration and shock-evaluation of human exposure to whole-body vibration. *Intl. Organization for Standardization, ISO*, *2631*.

Antonelli, D., Nesi, L., Pepe, G., & Carcaterra, A. (2019, June). A novel approach in Optimal trajectory identification for Autonomous driving in racetrack. In *2019 18th European Control Conf. (ECC)* (pp. 3267-3272). IEEE.

Aswani, A., Gonzalez, H., Sastry, S. S., & Tomlin, C. (2013). Provably safe and robust learning-based model predictive control. *Automatica*, *49*(5), 1216-1226.

Bellem, H., Thiel, B., Schrauf, M., & Krems, J. F. (2018). Comfort in automated driving: An analysis of preferences for different automated driving styles and their dependence on personality traits. *Transportation research part F: traffic psychology and behaviour*, *55*, 90-100.

Diels, C. (2014). Will autonomous vehicles make us sick? *Contemporary ergonomics and human factors. Taylor & Francis*, 301-307.

Donohew, B. E., & Griffin, M. J. (2004). Motion sickness: effect of the frequency of lateral oscillation. *Aviation, Space, and Environmental Medicine*, *75*(8), 649-656.

Easa, S. M., & Diachuk, M. (2020). Optimal Speed Plan for the Overtaking of Autonomous Vehicles on Two-Lane Highways. Infrastructures, 5(5), 44.

Elsner, J. (2018). Optimizing Passenger Comfort in Cost Functions for Trajectory Planning. *arXiv preprint arXiv:1811.06895*.

Epic Games. (2019). *Unreal Engine*. Retrieved from https://www.unrealengine.com.

Filip, J. (2018). Trajectory Tracking for Autonomous Vehicles.

Geng, K., & Liu, S. (2020). Robust Path Tracking Control for Autonomous Vehicle Based on a Novel Fault Tolerant Adaptive Model Predictive Control Algorithm. Applied Sciences, 10(18), 6249.

Hajizadeh, I., Hobbs, N., Sevil, M., Rashid, M., Askari, M. R., Brandt, R., & Cinar, A. (2020, May). Performance Monitoring, Assessment and Modification of an Adaptive MPC: Automated Insulin Delivery in Diabetes. In *2020 European Control Conference (ECC)* (pp. 283-288). IEEE.

Htike, Z., Papaioannou, G., Velenis, E., & Longo, S. (2020, May). Motion Planning of Self-driving Vehicles for Motion Sickness Minimisation. In *2020 European Control Conference (ECC)* (pp. 1719-1724). IEEE.

Iskander, J., Attia, M., Saleh, K., Nahavandi, D., Abobakr, A., Mohamed, S., . & Hossny, M. (2019). From car sickness to autonomous car sickness: A review. *Transportation research part F: traffic psychology and behaviour*, *62*, 716-726.

Kang, C. M., Lee, S. H., & Chung, C. C. (2014, October). Lane estimation using a vehicle kinematic lateral motion model under clothoidal road constraints. In *17th International IEEE Conference on Intelligent Transportation Systems (ITSC)* (pp. 1066-1071). IEEE.

Lambert, E., Romano, R., & Watling, D. (2019, May). Optimal path planning with clothoid curves for passenger comfort. In *Proceedings of the 5th Intl. Conf. on Vehicle Technology and Intelligent Transport Systems (VEHITS 2019)*,Vol.1, pp.609-615. SciTePress.

Luan, Z., Zhang, J., Zhao, W., & Wang, C. (2020). Trajectory Tracking Control of Autonomous Vehicle with Random Network Delay. IEEE Transactions on Vehicular Technology.

MATLAB. (2020). *version (R2020a)*. Natick, Massachusetts: The MathWorks Inc.

Mechanical Simulation Corporation. (2020). *Introduction to CarSim*.

Muske, K. R., & Rawlings, J. B. (1993). Model predictive control with linear models. *AIChE Journal*, *39*(2), 262-287.

Önkol, M., & Kasnakoğlu, C. (2018). Adaptive model predictive control of a two-wheeled robot manipulator with varying mass. *Measurement and Control*, *51*(1-2), 38-56.

Rajamani, R. (2011). *Vehicle dynamics and control*. Springer Science & Business Media.

Reason, J. T., & Graybiel, A. (1969). *Changes in subjective estimates of well-being during the onset and remission of motion sickness symptomatology in the slow rotation room* (Vol. 1083). US Naval Aerospace Medical Institute, Naval Aerospace Medical Center.

Road Safety Authority, (2011). The two-second rule, Government of Ireland.

Sivak, M., & Schoettle, B. (2015). *Motion sickness in self-driving vehicles*. University of Michigan, Ann Arbor, Transportation Research Institute.

Shi, J., Sun, D., Qin, D., Hu, M., Kan, Y., Ma, K., & Chen, R. (2020). Planning the trajectory of an autonomous wheel loader and tracking its trajectory via adaptive model predictive control. Robotics and Autonomous Systems, 103570.

Standard, B. S. I. (1987). 6841, Guide to Measurement and Evaluation of Human Exposure to Whole-Body Mechanical Vibration and Repeated Shock. *London, UK: BSI*.

Wu, J., Wang, Z., & Zhang, L. (2020). Unbiased-estimation-based and computation-efficient adaptive MPC for four-wheel-independently-actuated electric vehicles. Mechanism and Machine Theory, 154, 104100.

Yimer, T. H., Wen, C., Yu, X., & Jiang, C. (2020). A Study of the Minimum Safe Distance between Human Driven and Driverless Cars Using Safe Distance Model. *arXiv preprint arXiv:2006.07022*.